The 6th International Supercritical CO_2 Power Cycles Symposium
March 27-29, 2018, Pittsburgh, Pennsylvania

Test Rig Design for Large Supercritical CO_2 Turbine Seals

Aaron Rimpel
Southwest Research Institute
San Antonio, TX

Natalie Smith
Southwest Research Institute
San Antonio, TX

Jason Wilkes
Southwest Research Institute
San Antonio, TX

Hector Delgado
Southwest Research Institute
San Antonio, TX

Timothy Allison
Southwest Research Institute
San Antonio, TX

Rahul A. Bidkar
GE Global Research
Niskayuna, NY

Uttara Kumar
GE Global Research
Niskayuna, NY

Deepak Trivedi
GE Global Research
Niskayuna, NY

ABSTRACT

Feasibility studies have investigated utility-scale (450 MW_e) supercritical carbon dioxide (sCO_2) turbomachinery designs for closed-loop Brayton cycle applications. In order to take full advantage of the benefits of sCO_2 over other working fluids – namely, higher possible thermal cycle efficiency – it is necessary to advance the state-of-the-art of large-size turbine end seals. A new film-riding face seal design is under development for an application with an approximately 24 in. seal diameter, and a full-scale test rig is being designed to test this new seal. The seal and test rig are designed to restrict CO_2 leakage from supercritical conditions to near-atmospheric pressure with shaft speeds up to 3600 rpm. The present paper describes aspects of the new rig design, including the flow loop configuration and special operating scenarios, pressure casing design, and rotor design.

INTRODUCTION

Supercritical carbon dioxide (sCO_2) as the working fluid in closed-loop recompression Brayton cycles offers the possibility of higher thermal cycle efficiency compared to state-of-the-art ultrasupercritical steam cycles [Le Moullec 2013]. Conceptual studies have demonstrated the feasibility and approximate size requirements of the turbomachinery for utility-scale sCO_2 power cycles up to 450 MW_e [Bidkar et al. 2016a,b]. As identified in these studies, one of the significant technology gaps that must be addressed in order for utility-scale sCO_2 power cycles to realize the desired efficiency advantages is in the turbine shaft end seals. Despite the relative compactness of sCO_2 machinery compared to those using other working fluids, a utility-scale sCO_2 turbine shaft end seal would still need to be roughly 24 in. diameter. This means that the seals' effective clearance must be very small (e.g., 0.001 in. or less) in order to minimize efficiency-robbing leakage and be able to withstand differential pressures of over 1000 psi. It is noted that the performance penalty from this leakage is exacerbated by the unique characteristics of sCO_2, which is less of a concern for analogous seals in conventional gas or steam turbines. For example, Bidkar et al. [2016a] showed that using conventional turbine end seal technology (labyrinth seals) for this sCO_2 turbine would result in a decrease in cycle efficiency by 0.6-0.8 percentage points compared to using more advanced seals with order-of-magnitude lower leakage. Film-riding face seal technology would be relatively well-suited for this application; however, due to the size, pressure, and challenging manufacturing

considerations, such seals are not yet commercially available. Therefore, significant recent development has been focused on designing a new low-leakage face seal for this type of machinery [Bidkar et al. 2016c].

A previous paper [Rimpel et al. 2016] discussed the conceptual design of a test rig for testing this new sCO_2 seal. This was the result of an earlier phase of the current project funded by the U.S. Department of Energy. Current project activities include the detailed design of the new face seal technology, testing of a reduced-scale seal prototype, and the detailed design of the full-scale seal test rig – all of which are currently in-progress. Construction and commissioning of the full-scale test rig is planned for this year, and the test program is planned for completion in 2019. The scope of this paper is to present various aspects of the current full-scale test rig design.

RIG DESCRIPTION

Figure 1 shows the cross-section of the test rig (main view) along with an external view (inset). As shown in the cross-section, the main supply flow is brought into the center of the casing, and there are two identical test seals (except for direction of rotation) mounted on the case heads and interfacing with a disk on the center of the rotor. The supply flow actually enters the case barrel and passes through a swirl ring, which imparts tangential velocity in the so-called "upstream cavity" (indicated by red dashed lines) with the purpose of reducing windage loss. Secondarily, the swirling flow enhances heat transfer for cooling the test rig, and a large portion of the supply flow is returned to the flow loop where the heat is rejected through coolers. The upstream cavity is common to both test seals and has a design pressure just higher than the critical pressure of CO_2, or 75 bar (1088 psi). Leakage through the test seals flows into the "downstream cavities" (indicated by blue dashed lines), which are vented axially through ports in the case heads and are piped through independent flow meters before discharging to atmosphere. The pressure in the downstream cavities can be near-atmospheric or back-pressured up to 10 bar (145 psi). More details about the flow loop are presented in a later section.

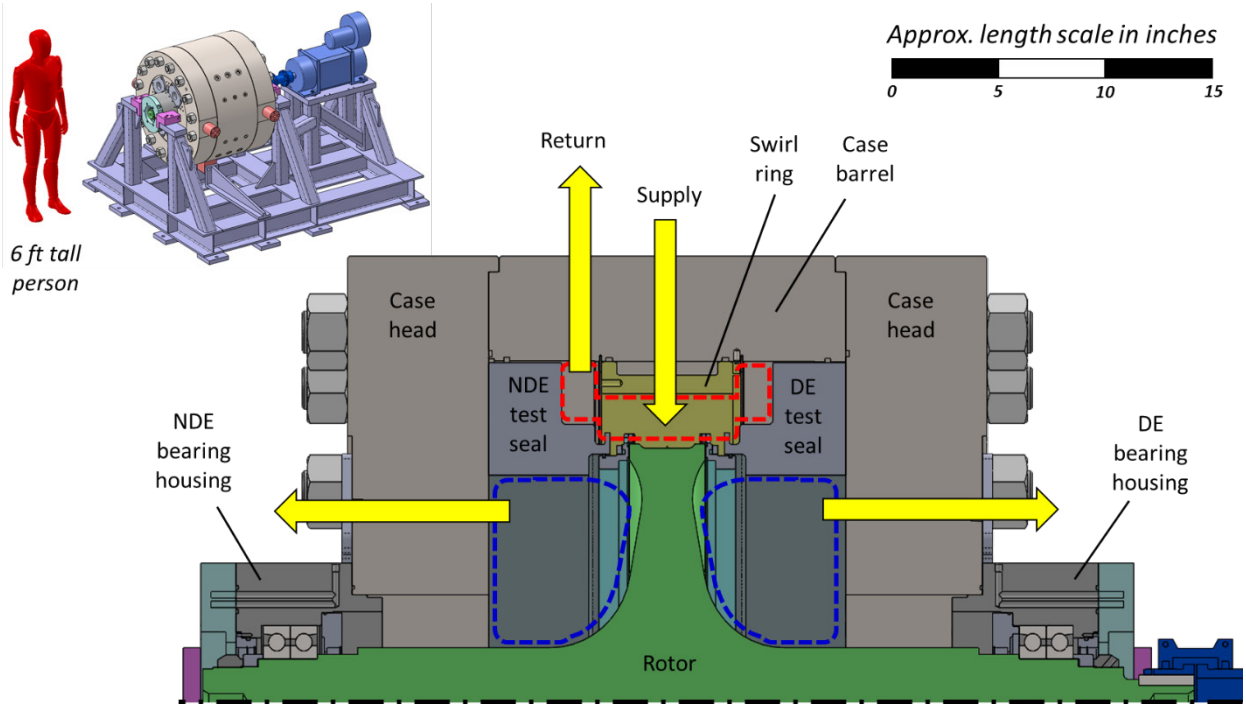

Figure 1. Test Rig Views

The symmetry of the case construction ensures that response to pressure and temperature – i.e., deflections, etc. – should likewise be symmetric. Also, the back-to-back seal arrangement with seals that leak at the same rates ensures a thrust-balanced rotor since the downstream cavities should be at the same pressure. Nevertheless, as shown in a later section, the loop incorporates the ability to independently back-pressure each seal's discharge line as a means to control thrust load in the event that leakages are not identical. Another reason for incorporating two test seals, as opposed to one test seal on one side with another type of currently-available seal technology on the other, is that leakage through the other seal would be significantly larger. As described later, the total leakage through these seals needs to be made up by the flow loop, so it should be minimized. Symmetry is also carried out in the rotor design, where the disk is positioned equally from the drive end (DE) and non-drive end (NDE) bearings. The DE bearings also serve as the thrust bearing for the rotor, while the NDE bearings can float to account for relative rotor-stator deflections (e.g., thermal growth). Finally, the rotor is directly coupled to a variable speed motor, which has a design speed of 3600 rpm. Table 1 summarizes the main test rig design parameters.

Table 1. Test Rig Design Parameters

Quantity	Value
Seal diameter	24 in.
Shaft design speed	3600 rpm
Supply temperature to rig (max)	400 °F
Upstream cavity pressure	75 bar (1088 psi)
Downstream cavity pressure (max)	10 bar (145 psi)

CASING DESIGN

The functions of the casing are to contain the high-pressure CO_2 required for testing the seals and provide position control for the seals during operation. The latter function is actually the limiting requirement – i.e., position control necessitates larger wall thicknesses than pressure containment. Under normal operation, the upstream cavity experiences the highest pressure, and the downstream cavities have relatively low pressure. As shown in the discussion of the flow loop, the downstream cavities have pressure protection at 200 psi, which significantly decreases the loads on the case heads and bolts of the pressure vessel in the event of a seal failure.

The casing was designed using finite element analysis (FEA) according to ASME Boiler and Pressure Vessel Code, Section VIII, Division 2, Part 5. Nonlinear elastic-plastic analysis, which uses 2.4X pressure load, showed that plastic strain was effectively nonexistent in the bulk of the casing material. Figure 2 shows an earlier version of the vessel design and the plot of total equivalent plastic strain (ϵ_{peq}) divided by the limiting triaxial strain (ϵ_L). Note that the maximum value is in the region of the threads and is well below the limit (0.066 < 1). An additional nonlinear analysis reviewed the 1X pressure loads for hydrostatic test conditions followed by alternating unloading and loading at the rated vessel pressure. This analysis evaluated whether additional plastic strain accumulates with each loading cycle (known as ratcheting). The results showed that equivalent plastic strain was identical for consecutive loading cycles, indicating that ratcheting would not occur and the design is satisfactory from a pressure design point of view.

As previously mentioned, deflection control actually limits the casing design. All the Boiler and Pressure Vessel Calculations, like shown in Figure 2, were performed on an earlier iteration of the rig design, which

had thinner walls. The walls were actually thickened approximately 75% to their current state (see Figure 1) in order to limit tapering deflections at the seal mounting face to less than 0.0005 in.

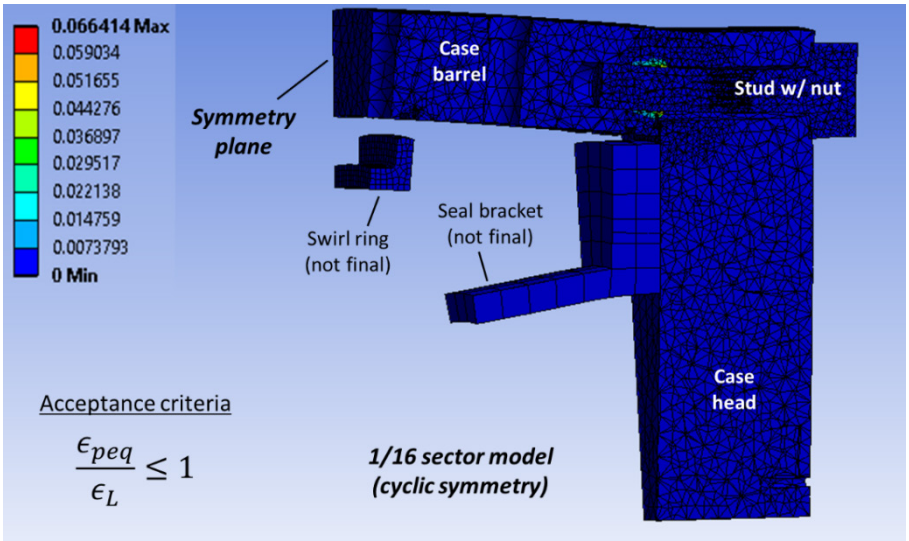

Figure 2. Elastic-Plastic Analysis Solution: Equivalent Plastic Strain Divided By Limiting Triaxial Strain

ROTOR DESIGN

As shown in Figure 1, the rotor design is a single piece shaft with integral disk. This design was determined after significant analysis and evaluation of competing designs. An early assumption was that an assembled or multi-piece rotor (i.e., separate shaft and disk) would reduce cost risk to the project because: (a) raw material billets or forgings in cylinder and disk shapes would have less machining time/waste than a large cylinder fitting the volume of the entire rotor, and (b) replacing a disk damaged beyond repair would be less costly than replacing an entire rotor. Before this assumption could be verified or disproven, a relatively mature design was required in order to obtain realistic manufacturing feedback and quotes for both single and multi-piece rotor designs.

The main challenges of a multi-piece rotor design are the requirement that the disk remains rigidly attached to the shaft and the requirement for symmetry in deflections of the face seal surfaces at the disk outer diameter (due to the back-to-back test seal arrangement). Since a disk has large inertia at a larger diameter than the shaft, a disk would grow radially more than the shaft due to thermal and centrifugal loading. As such, a disk-to-shaft joint would need to be a pilot fit with the male feature on the disk so the joint could grow tight during operation. The opposite joint (i.e., female feature on disk) would require an impractically large assembly interference fit to prevent the joint from growing loose.

Figure 3a shows a flange concept with the pilot fit having the male feature on the disk. Although deflections due to solely centrifugal loads could be made symmetric with the flange design concept, thermal loads on the asymmetric disk and shaft geometry created significant asymmetry, especially for ranges of thermal boundary conditions. A strictly symmetric geometry, such as the tie bolt rotor design in Figure 3b, was the only way to guarantee symmetric deflections due to both centrifugal and thermal loading. For the tie bolt rotor design, the disk's burst speed was evaluated using the Hallinan criterion [Barack and Domas 1975] and determined to have a burst margin (stress at burst to stress at operating condition) of 6.6. In terms of speed, the operating speed would only be 39% of the burst speed. Both of these metrics indicate a satisfactory design.

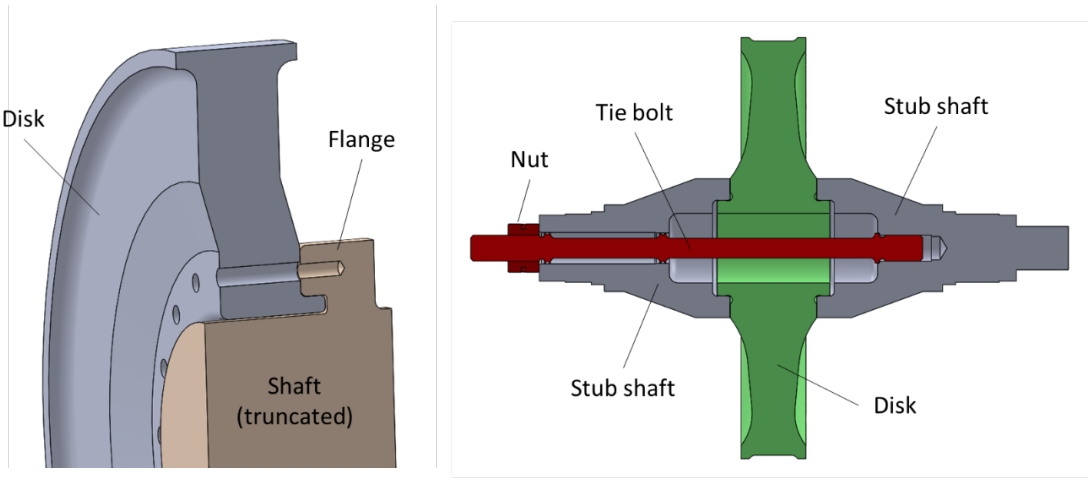

(a) Flange Disk Concept (b) Tie Bolt Rotor Design

Figure 3. Multi-Piece Rotor Concepts Evaluated, Not Selected

Finally, the tie bolt rotor design (Figure 3b) was compared with an equivalent solid rotor design on a cost basis. A key assumption for the tie bolt rotor design was that the rotor would need to go through an assembly machining step in order to provide suitable accuracy (runout, perpendicularity) at the face seal surfaces with respect to the bearing surfaces. Quotes from multiple vendors for both manufacturing options were obtained for a realistic assessment of the relative costs of the two options. Ultimately, the cost of single-piece rotor forgings (ASTM A473, Type 410) were found to be less significant than originally assumed, and fewer separately-machined parts greatly simplifies manufacturing, so the single-piece rotor was selected. Also, the single-piece rotor has lower stresses, which increased burst margin to over 8.0.

A key feature of the rotor design from the conceptual design phase [Rimpel et al. 2016] was that the operation was sub-critical – i.e., operating speed below the first critical speed – which simplifies operation and minimizes concern of instability. Figure 4 presents the unbalance response plots for the current design using four times the API balance specification [API 617] applied to the shaft – both unbalance mass and the response are located at the center of the disk. The unbalance response, which includes a compliance model for the foundation, shows that the rotor design is sub-critical with a separation margin of nearly 100%, which exceeds API requirements.

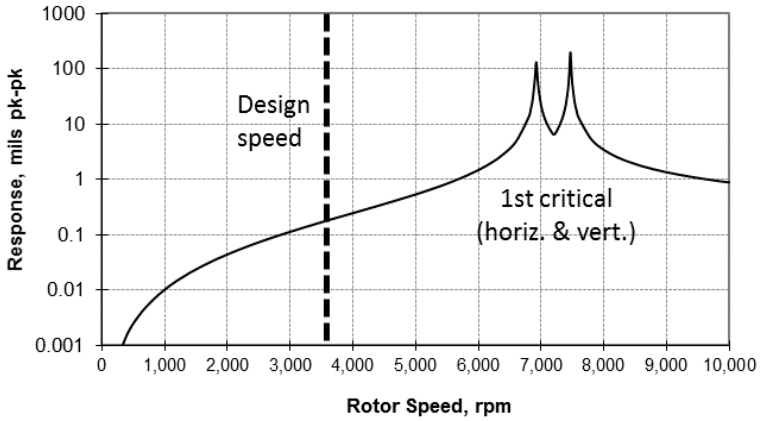

Figure 4. Unbalance Response at Disk Center with 4X API Unbalance

FLOW LOOP

The test rig flow loop is shown in Figure 5. As indicated, key elements of an existing sCO_2 flow loop [Moore et al. 2018] are being leveraged for the new facility. Notably, these include a dense phase CO_2 pump, heater, heat exchangers, miscellaneous piping and valves, etc. The existing loop was designed to supply a sCO_2 turboexpander with CO_2 up to approximately 1300°F (700°C) and 3400 psi (240 bar), which exceeds the current requirements. In the modification for the current rig, the turboexpander is bypassed and replaced with new loop components, as shown. The loop has open- (Line B) and closed-loop (Line C) sections: the open loop essentially involves the leakage flow through the test seals, while the closed loop is primarily a cooling circuit for the rig at the high-pressure supply (recall discussion in the Rig Description section). Make-up flow equaling the leakage rate through the seals will be continually supplied to the suction side of the CO_2 pump for the duration of a test. Flow rates will be measured up- and downstream of the rig to quantify leakage through the main seals as well other leakage paths and, together with various pressure and temperature measurements, to monitor the performance of the rig.

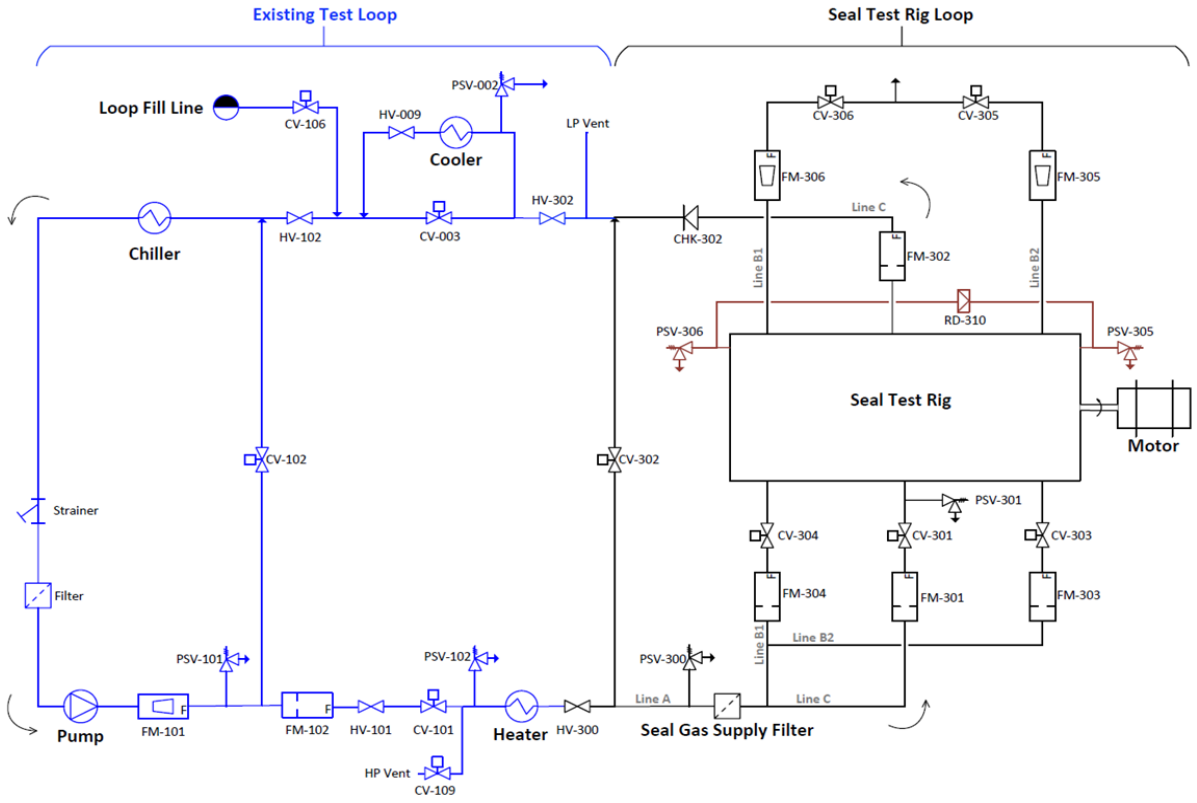

Figure 5. Flow Loop Schematic

Compared to other sCO_2 turbomachinery test programs [Wilkes et al. 2016, Moore et al. 2018, McClung et al. 2018], the operating conditions of this rig are not particularly challenging, mainly because temperatures are significantly lower. As such, material selection and pipe sizing is relatively straightforward. Because of the concern for contamination due to corrosion particles, all flow elements upstream of the rig are 316 stainless steel. However, downstream elements could be carbon steel to reduce cost and because filters in the loop are able to provide protection from any corrosion contamination propagating to the test seals. Most notably, the filter immediately upstream of the rig (see Figure 5) is similar to what would be used for a dry gas seal supply (filtration fineness of 3 µm).

A flow network analysis was completed, modeling all aspects of the seal test loop, accounting for pressure drops throughout the system for frictional losses through pipe, elbows, tees, etc., and permanent pressure drops across flow meters and control valves. Real gas properties were accounted for using the REFPROP material database [Lemmon et al. 2007]. Analysis using the design operating conditions was completed, and failure scenarios were analyzed to confirm maximum design pressures for the pressure vessel and thrust load on the shaft. One such scenario is the catastrophic failure of one of the test seals, which would expose its corresponding downstream cavity to higher pressure and create a larger pressure differential across the shaft (thrust load). The rest of this section highlights the analysis of the rig at design conditions as well as the aforementioned failure scenario and mitigation approach.

The initial analysis modeled the design operating condition. This allowed for an estimation of pressure drops through the system, approximate valve positions, and an equivalent loss factor across the test seals. Table 2 summarizes the main flow elements depicted in Figure 5 along with their major flow properties. Values highlighted in grey were constraints for the specific analysis case, while the non-highlighted values were calculated results of the analysis. At present, mass flow rates are proprietary, so they are normalized by the flow through Line A. Pressures upstream of the swirl ring supply and Lines B1 and B2 upstream of the test rig are also proprietary at this time and not able to be published. This analysis requires iteration to match the pressure constraints where Lines B1 and B2 tee together and at the open-loop vent (ambient pressure). Pressure drops are calculated through each element with K loss factors (for tees, elbows, reducers) and friction factors (for pipe lengths). Larger pressure drops are applied at the control valves to meet the required upstream and downstream pressures. The valves are modeled as orifice restrictions, and the bore diameter is calculated to be consistent for the design condition “throttle position”. Additionally, based on geometry and pressures, K factors are calculated for the internal seal and swirl ring flow blockages. Finally, for the design case, this analysis provides an estimate of the pressure conditions that will be required from the existing test loop with the dense phase CO_2 pump; these are the supply pressure for Line A and the return pressure for Line C. The results of this analysis in terms of pressure loss are illustrated in Figure 6.

Within this analysis, two flow parameters were monitored at each element: pressure drop and choked flow condition. Generally, it is good practice to minimize the permanent pressure drop across orifice flow meters. For the current application, it was especially critical for the upstream lines. The main concern with large pressure drops across flow elements is condensation, which would lead to two potential issues. Firstly, liquid condensation is a dangerous contaminate for small running clearance seals [Day and Allison 2016, Allison et al. 2018]. Secondly, the formation of condensation could potentially affect the *vena contracta* diameter of the orifice flow meter, rendering the discharge coefficient calibration inaccurate and cause high uncertainty of the flow rate measurement.

The results from the design condition analysis were used as constraints for the failure scenarios. For the purposes of the analysis, it was assumed that in the event of a catastrophic seal failure on one side of the rig, the control valves would remain in their current position, and supply pressure from the pump would remain nearly constant. In other words, it was assumed the valves could not be controlled fast enough to mitigate the transient event, and the pump has infinite mass flow potential. The former assumption is fairly realistic, but the latter is certainly conservative. In reality, increased mass flow would be at the cost of lower supply pressure. The K loss factors calculated for the seal and swirl ring were used to estimate the flows through those elements, and intermediate pressures and the flow rates were allowed to change to satisfy the constraints.

Table 2. Flow Network Analysis Major Parameters.
(Gray Indicates a Constraint, While White Indicates a Calculated Parameter)

Tag	Parameter Description	Units	Design Case	Failure Scenario 1	Failure Scenario 2
Line A	Mass Flow (norm.)	-	1.000	1.053	1.588
	Supply Pressure	-	P_{supply}	P_{supply}	P_{supply}
CV-301	Mass Flow (norm.)	-	0.817	0.613	0.954
	Restriction Bore Diameter Ratio	-	0.315	0.315	0.315
CV-303	Mass Flow (norm.)	-	0.093	0.353	0.551
	Restriction Bore Diameter Ratio	-	0.472	0.472	0.472
CV-304	Mass Flow (norm.)	-	0.093	0.087	0.084
	Restriction Bore Diameter Ratio	-	0.472	0.472	0.472
Swirl Ring	Upstream Pressure	*bar*	83.0	101.0	51.0
	Downstream Pressure	*bar*	75.0	97.5	13.8
	K factor	-	1.86	1.86	1.86
Seal DE	Downstream Pressure	*bar*	10.0	97.5	13.8
	K factor	-	4.46	*NA*	*NA*
Seal NDE	Downstream Pressure	*bar*	10.0	17.3	16.8
	K factor	-	4.46	4.46	4.46
Line C DS	Mass Flow (norm.)	-	0.712	*NA*	*NA*
	Return Pressure	*bar*	70.0	*NA*	*NA*
CV-305	Mass Flow (norm.)	-	0.146	0.913	0.111
	Restriction Bore Diameter Ratio	-	0.165	0.165	0.165
CV-306	Mass Flow (norm.)	-	0.146	0.140	0.135
	Restriction Bore Diameter Ratio	-	0.165	0.165	0.165
Exit Tee	Pressure Match	-	$\Delta P = 0$	$\Delta P = 0$	$\Delta P = 0$
Exit	Ambient Pressure	*bar*	1	1	1

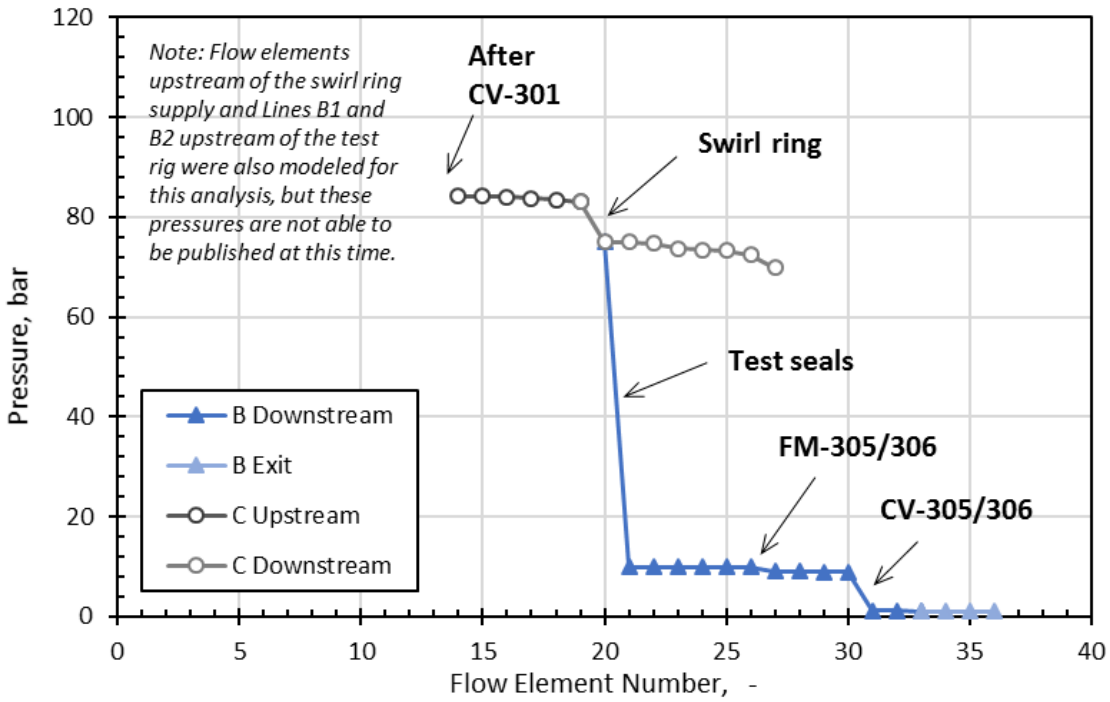

Figure 6. Pressure Conditions Through Seal Test Rig – Design Condition

Failure Scenario 1 considers a case where the rig and seal rig loop have no protection elements, such as pressure safety valves (PSVs) or rupture discs. In other words, the red elements in Figure 5 (PSV-305, PSV-306, and RD-310) were assumed to not be in the loop. For the purpose of the analysis, the DE seal was made to be the failed seal. The goal was to estimate what pressure would build up in the cavity downstream of the seal (P_{DS}) if a seal were to fail. This drives two key criteria: the pressure rating for the pressure vessel containing the seal and the differential pressure between the DE and NDE of the rig. The results for this scenario are summarized in Table 2 and Figure 7. Notice that the resulting pressure in the downstream cavity on the failed seal side was unreasonably high, requiring significantly more load resistance from the casing head bolts. Moreover, the resulting 80 bar (1160 psi) pressure differential between the two sides of the rotor would overwhelm the thrust bearing. It is also noted that the pressure to the swirl ring has increased from 83 bar to over 100 bar due to a reduction in mass flow, which decreases the pressure drop through CV-301.

The results from Failure Scenario 1 motivated a design change to include the protection elements illustrated in red in Figure 5 (PSV-305, PSV-306, and RD-310). Failure Scenario 2, models the same DE seal failure, but with the PSV-305 egressing flow to reduce the pressure in the rig (PSV-306 and RD-310 are not actively modeled in this case). Each PSV was sized to the supply flow rate and a set pressure of 200 psi (13.8 bar). The results for this scenario are summarized in Table 2 and Figure 8, and there are several observations worth pointing out. First, flow rate increased significantly through CV-301, resulting in only about 50 bar being supplied to the swirl ring. Next, the pressure difference between the two downstream cavities is only 3 bar (44 psi), which results in a thrust force within the capacity of the thrust bearing. However, this is conservative since the predictions show the maximum pressure on the NDE side exceeds the PSV set point (not modeled). In the actual failure scenario, the PSVs on both sides would be activated, and the pressures would be equal. Moreover, the rupture disk (RD-310) would provide an additional safety measure in case the downstream lines (Lines B1 and B2) are unable to balance the pressure fast enough.

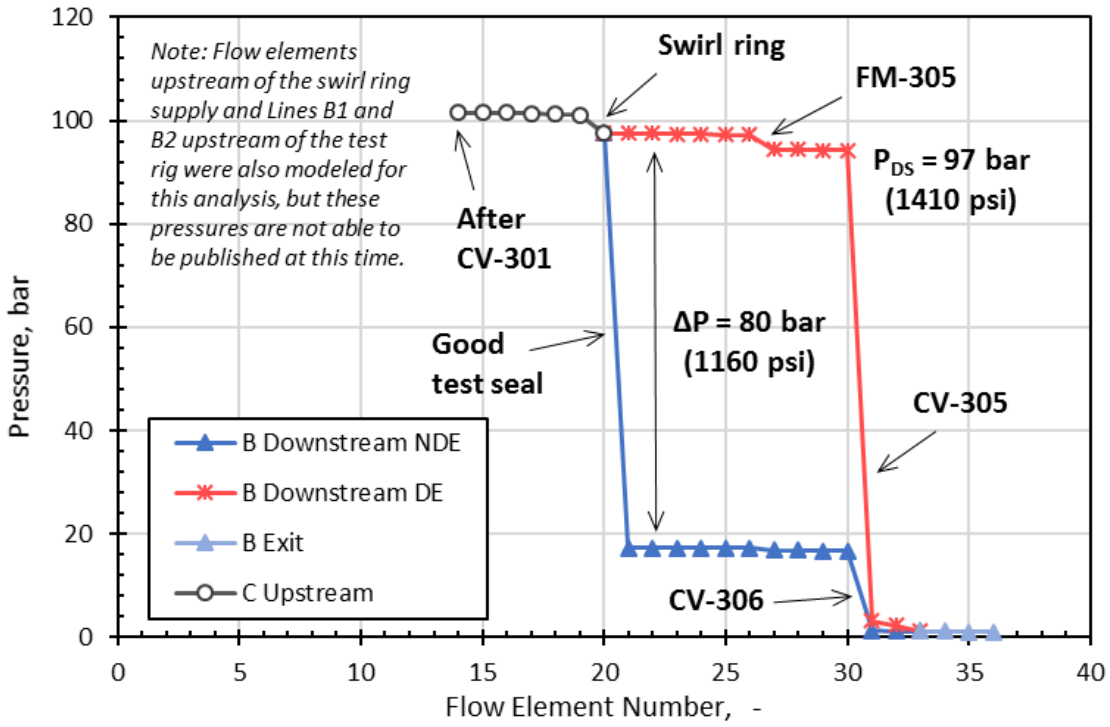

Figure 7. Pressure Conditions Through Seal Test Rig – Failure Scenario 1, No Protection

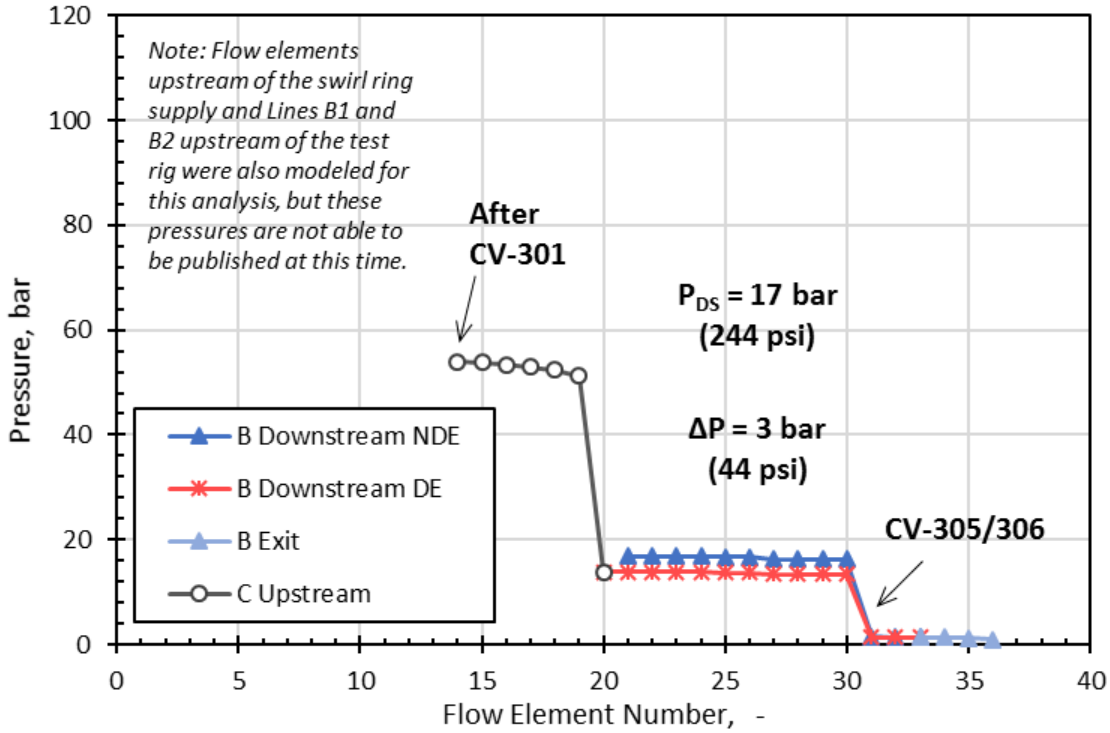

Figure 8. Pressure Conditions Through Seal Test Rig – Failure Scenario 2, PSV on Downstream Cavity

SUMMARY AND CONCLUSIONS

Several aspects of the design of a test rig for a new film-riding face seal were presented. The new seal technology is being developed for utility-scale (450 MW_e) sCO_2 turbines, which require improved leakage performance than the current state-of-the-art at the required sizes, pressures, and temperatures. The test rig is configured to test two seals in a back-to-back configuration, which facilitates a thrust-balanced rotor design and minimizes leakage flow to be made-up by the test loop. The test rig casing was designed for pressure containment according to ASME Boiler and Pressure Vessel Code, but the limiting factor of the design was deflection control, which required significantly thicker walls. The rotor was designed to be a monolithic structure as opposed to a multi-piece assembly. A single-piece rotor has a higher burst margin, is less complicated to manufacture, and does not have significant cost disadvantages compared to a multi-piece design. From a rotordynamics perspective, the design is subcritical with over 100% separation margin. Finally, the test loop utilizes an existing sCO_2 loop and features open- and closed-loop sections. The open-loop involves the leakage flow through the test seals, which must be continually made-up by the loop during a test, while the closed-loop cools the rig at the seal supply pressure. Analyses verified that excessive downstream cavity pressure and thrust load would be mitigated in the event of a catastrophic seal failure scenario.

ACKNOWLEDGEMENT

This material is based upon work supported by the U.S. Department of Energy under Award Number DE-FE0024007. The authors want to thank Dr. Seth Lawson at U.S. Department of Energy – National Energy Technology Laboratory for his support and guidance during this program. We are thankful to Dr. Jeffrey Moore of Southwest Research Institute, and Dr. Bugra Ertas, Mr. Jason Mortzheim, and Mr. Chris Wolfe of the General Electric Company for discussions related to the test rig.

DISCLAIMER

REFERENCES

Allison, T., Moore, J., Hofer, D., Tower, M.D., Thorp, J., 2018, “Planning for Successful Transients and Trips in a 1 MW_e-scale High-Temperature sCO_2 Test Loop,” Paper No. GT2018-75873, to be presented at ASME Turbo Expo 2018, June 11-15, Oslo, Norway.

API 617, 2002, “Axial and Centrifugal Compressors and Expander-Compressors for Petroleum, Chemical and Gas Industry Services,” Seventh Edition, American Petroleum Institute, Washington, D.C.

Barack, W.N., and Domas, P.A., 1975, “An Improved Turbine Disk Design to Increase Reliability of Aircraft Jet Engines,” NASA Report CR-135033.

Bidkar, R. A., Mann, A., Singh, R., Sevincer, E., Cich, S., Day, M., Kulhanek, C. D., Thatte, A., Peter, A. M., Hofer, D., and Moore, J., 2016, "Conceptual Designs of 50 MW_e and 450 MW_e Supercritical CO_2 Turbomachinery Trains for Power Generation from Coal. Part 1: Cycle and Turbine," The 5th International Supercritical CO_2 Power Cycles Symposium, March 28-31, San Antonio, TX.

Bidkar, R. A., Musgrove, G., Day, M., Kulhanek, C. D., Allison, T., Peter, A. M., Hofer, D., and Moore, J., 2016, "Conceptual Designs of 50 MW_e and 450 MW_e Supercritical CO_2 Turbomachinery Trains for Power Generation from Coal. Part 2: Compressors," The 5th International Supercritical CO_2 Power Cycles Symposium, March 28-31, San Antonio, TX.

Bidkar, R. A., Sevincer, E., Wang, J., Thatte, A. M., Mann, A., Peter, M., Musgrove, G., Allison, T., and Moore, J., 2016, "Low-Leakage Shaft End Seals for Utility-Scale Supercritical CO_2 Turboexpanders," Paper No. GT2016-56979, Proceedings of ASME Turbo Expo 2016, June 13-17, Seoul, South Korea.

Day, M. and Allison, T., 2016, "Analysis of Historical Dry Gas Seal Failure Data," Paper No. GT2016-57076, Proceedings of ASME Turbo Expo 2016, June 13-17, Seoul, South Korea.

Le Moullec, Y., 2013, "Conceptual Study of a High Efficiency Coal-Fired Power Plant with CO_2 Capture Using a Supercritical CO_2 Brayton Cycle," Energy, 49, pp. 32-46.

Lemmon, E. W., Huber, M. L., and McLinden, M. O., 2007, "NIST Standard Reference Database 23: Reference Fluid Thermodynamic and Transport Properties—Refprop, Version 8.0," National Institute of Standards and Technology, Gaithersburg, MD.

McClung, A., Kutin, M., and Hofer, D., 2018, "Capabilities of the 10 MW_e sCO_2 STEP Test Facility," The 6th International Supercritical CO_2 Power Cycles Symposium, March 27-29, Pittsburgh, Pennsylvania.

Moore, J., Cich, S., Wade, J., and Hofer, D., 2018, "Commissioning of a 10 MW_e Supercritical CO_2 Turbine," The 6th International Supercritical CO_2 Power Cycles Symposium, March 27-29, Pittsburgh, Pennsylvania.

Rimpel, A., Delgado, H., Allison, T., Cich, S., Day, M., Bidkar, R., Sevincer, E., Thatte, A., and Wang, J., 2016, "Conceptual Test Rig Design for Full Size Utility Scale Supercritical CO_2 Turbine Shaft End Seals," The 5th International Supercritical CO_2 Power Cycles Symposium, March 28-31, San Antonio, TX.

Wilkes, J., Allison, T., Schmitt, J., Bennett, J., Wygant, K., Pelton, R., and Bosen, W., 2016, "Application of an Integrally Geared Compander to an sCO_2 Recompression Brayton Cycle," The 5th International Supercritical CO_2 Power Cycles Symposium, March 28-31, San Antonio, TX.

AUTHOR BIOGRAPHIES

Mr. Aaron Rimpel is a Senior Research Engineer and the Machine Design Coordinator in the Rotating Machinery Dynamics Section at Southwest Research Institute in San Antonio, TX. His experience includes rotordynamic analyses, design and testing of bearings and seals for conventional and oil-free turbomachinery, aerodynamic performance testing, supercritical CO_2 power cycle applications, and test rig design. Mr. Rimpel received a M.S. in Mechanical Engineering from Texas A&M University in 2008 with a focus on gas bearings and rotordynamics.

Dr. Natalie Smith is a Research Engineer in the Rotating Machinery Dynamics Section at Southwest Research Institute in San Antonio, TX. Her research experience at SwRI includes aerodynamic design, analysis, and testing of turbomachinery for various applications including power generation, oil and gas, and supercritical CO_2. She earned her Ph.D. in Aeronautics and Astronautics from Purdue University.

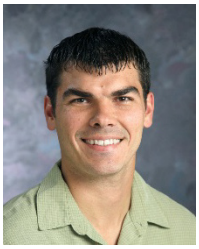

Dr. Jason Wilkes is a Senior Research Engineer in the Rotating Machinery Dynamics Section at Southwest Research Institute in San Antonio, TX. His experience at SwRI includes design and construction of various test rigs, predicting lateral and torsional rotordynamic analyses, bearings and seals, and auxiliary bearing dynamics following failure of active magnetic bearing-supported turbomachinery. Dr. Wilkes holds a B.S., M.S., and Ph.D. in Mechanical Engineering from Texas A&M University, where he studied at the Turbomachinery Laboratory for 6 years.

Mr. Hector Delgado is a Group Leader of the Machinery Services Section at Southwest Research Institute in San Antonio, TX. His experience includes turbomachinery root cause failure analyses, rotordynamics studies, machinery field testing, structural and thermal analyses, design for pipeline pulsation and vibration control and mitigation, blade and impeller dynamics analysis, and fatigue remaining life prediction. Mr. Delgado received B.S. and M.S. degrees in Mechanical Engineering from the University of Nuevo Leon in Mexico and The University of Texas at San Antonio, respectively.

Dr. Timothy Allison is the manager of the Rotating Machinery Dynamics Section at Southwest Research Institute in San Antonio, TX. His research at SwRI includes finite element analysis, modal testing, instrumentation, and performance testing for applications including high-pressure turbomachinery, centrifugal compressors, gas turbines, reciprocating compressor valves, and test rigs for rotordynamics, blade dynamics, and aerodynamic performance. He holds a Ph.D. in Mechanical Engineering from Virginia Polytechnic Institute and State University.

Dr. Rahul Bidkar is a Mechanical Engineer at GE Global Research Center in Niskayuna, NY and works in the area of turbomachinery seals. At GE, Dr. Bidkar is the Principal Investigator for a DOE program to develop low leakage seals for utility-scale sCO_2 turbines. Dr. Bidkar has led development of several film-riding turbomachinery seals with applications to GE's aircraft engines, gas turbines, and steam turbines as well as hydrophobic coatings development work for fluid drag reduction. Prior to joining GE, Dr. Bidkar received his Ph.D. in Mechanical Engineering from Purdue University in 2008. Dr. Bidkar has authored over 19 technical papers and about 20 patents/patent applications in the field of film-riding turbomachinery seals.

Dr. Uttara Kumar is a Lead Mechanical Engineer at GE Global Research in Niskayuna, NY. She received her Ph.D. in mechanical engineering from the University of Florida. At GE, her focus has been design and analysis (aeromechanics, rotordynamics, structural dynamics) for gas turbine and supercritical CO_2 turbine components and vibration testing.

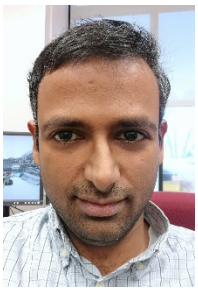

Dr. Deepak Trivedi is a Mechanical Engineer at GE Global Research Center in Niskayuna, NY. He received his Ph.D. in Mechanical Engineering from Penn State University. His research at GE includes developing sealing technologies and test rigs for severe conditions of temperature, pressure, speed, and transients. Applications include contacting and non-contacting seals for turbomachinery as well as elastomeric seals for subsea oil and gas applications. He has authored over 15 technical papers, 20 patent applications with 4 granted patents.